

EXPERIMENTAL TECHNIQUES FOR FISSION DATA MEASUREMENTS

Hans-Hermann J. Knitter and Carl Budtz-Jørgensen\*

Commission of the European Communities,  
 Joint Research Centre - Geel-Establishment,  
 Central Bureau for Nuclear Measurements, 2440 Geel, Belgium.

**Abstract:** Progresses in the development of experimental techniques for fission data measurements are reviewed briefly. This review comprises techniques for the preparation of special compound nuclei leading to fission (fission entrance) as well as experimental techniques which permit the measurement of the diversified characteristics of the emitted radiations in fission (fission exit). The latter developments are only considered when also other parameters than yield, mass, and energy of fission fragments are determined. Ionization chambers developed at CBNM are described in more detail. A simple ionization chamber with frische grid was used to determine fission layer characteristics, e.g. the number of fissile nuclei of a sample with an accuracy of smaller than 0.3%. A twin ionization chamber is described which has an advantageous  $2 \times 2\pi$  solid angle for fission fragment detection, a timing jitter of less than 0.7 ns, an energy resolution of smaller than 500 keV for fission fragments, and an angular resolution of  $\Delta \cos\theta < 0.05$ . Also the nuclear charge distribution of the fragments can be determined. A pulse pile-up rejection circuit was developed, which reduces pulse pile-up by more than a factor 30. This detector is well suited for correlation measurements between fission fragment parameters, like mass and total kinetic energy, and the characteristics of the different radiations emitted from the fragments. This type of ionization chamber was successfully used in several experiments and some results are shown to demonstrate its capabilities.

(Fission fragment detectors, neutron-fragment correlations, ternary fission)

1. Introduction

The process of nuclear fission is now known since about half a century, and still, nuclear fission is a very interesting and challenging subject of investigation, because it is by far not understood in all its aspects. Moreover, fission is a very complex phenomenon, where a heavy nucleus, by change of its shape and

structure, undergoes a completely new mass rearrangement resulting in two independent new nuclei of generally different size, accompanied by the emission of a few secondary particles and  $\gamma$ -radiation. This mass rearrangement leads to the well known large energy release in fission. The complexity of this process is illustrated in fig. 1. The evolution of the geometrical nuclear configuration is accompanied by considerable

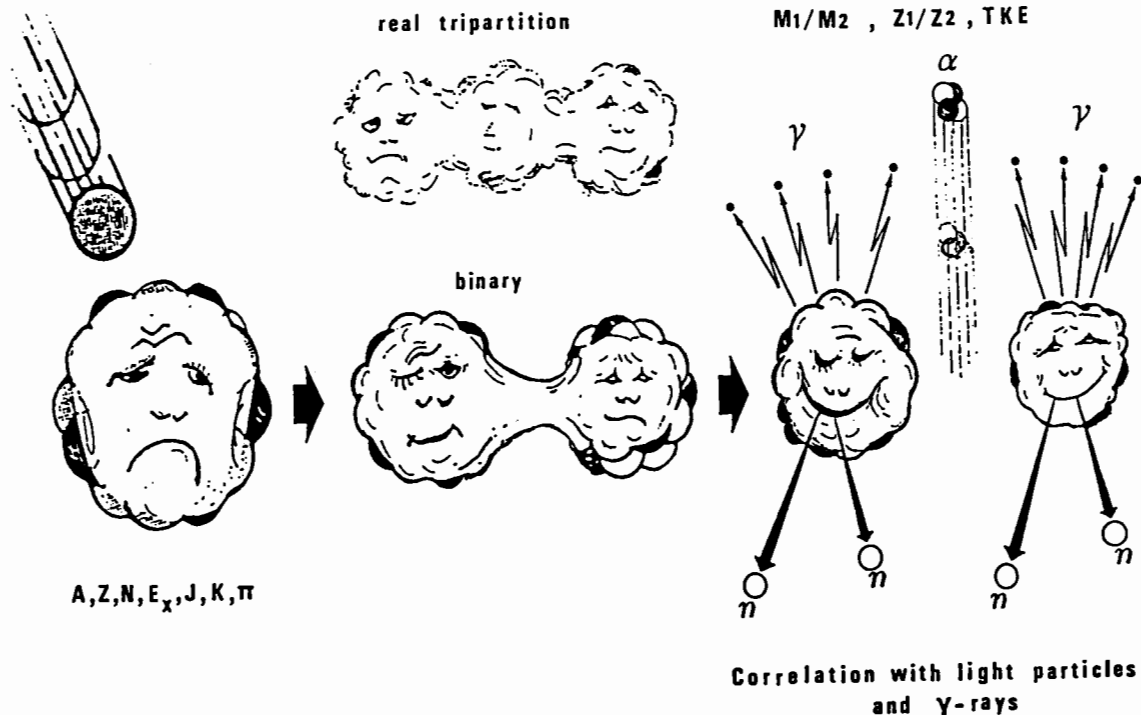


Fig. 1 : A special view on fission

Present address:

• Danish Space Research Institute, DK-2800  
 Lyngby, Denmark

changes of the nuclear potential energy, which in general is displayed by potential energy landscapes, i.e. mappings of the shell- and pairing-corrected liquid drop potential as function of deformation coordinates. The sequence of shapes of the fissioning nucleus described by elongation-, neck-, and mass asymmetry-parameters is characterized by a path in the multi-dimensional potential energy landscape. This motion to scission is also affected by inertia and viscosity of the fissioning nuclear matter.

From fig. 1 it is seen that the compound systems can be already very different in proton and neutron numbers  $Z$  and  $N$ , respectively, as well as in the excitation energy  $E_x$  and in the usual quantum numbers  $J$ ,  $K$  and  $\pi$ . In order to study the fission parameters from a large variety of nuclear compound species one must find new techniques for their preparation. Two examples of techniques will be reported, which were applied successfully in the preparation of very special and exotic fissioning nuclei.

In order to obtain a complete description of the fission process of a specific compound system all parameters should be measured. Therefore, during the last years many of the experiments became more complex and it was tried to measure simultaneously as many fission parameters as possible. Fig. 1 indicates schematically what kind of parameters are meant. A few of the experiments will be reviewed where more than the light and heavy fission fragment energies are measured. It is however not the place and not the time here to be very detailed and exhaustive.

## 2. Preparation of special nuclei for fission studies.

The preparation of special nuclei extends the variety of fissioning specimen undergoing fission and can give insight in their different structures.

### 2.1. Production of heaviest spontaneously fissioning elements.

In measurements during the last years Hulet et al./1,2,3/ measured the mass and kinetic energy partitioning in the spontaneous fission of  $^{258}\text{Fm}$ ,  $^{259}\text{Md}$ ,  $^{260}\text{Md}$ ,  $^{258}\text{No}$  and of the isotope  $^{260}\text{[104]}$ . The surprise of these measurements was that all of them fissioned with symmetric mass distributions, producing two energetic components. The authors interpreted this as a mixture of liquid-drop-like and fragment shell directed symmetric fission. These important experimental results for the understanding of fission were not anticipated by theory.

The very short-lived nuclides, 1.2ms  $^{258}\text{No}$  and 20ms  $^{260}\text{[104]}$  were produced in fusion reactions of 68 MeV  $^{13}\text{C}$  ions with  $^{248}\text{Cm}$  and of 81 MeV  $^{15}\text{N}$  ions with  $^{249}\text{Bk}$ , respectively. Recoil products emerging from the cyclotron target were stopped in a band of thin Al foils mounted on a rim of a 30 cm diameter wheel that spun up to 5000 rpm. These foils, when rotated, passed opposing banks of surface barrier detectors, which measured the energies of the coincident fragments. With fission event rates of 5 to 8 per hour 382  $^{258}\text{No}(\text{sf})$  events together with 59  $^{256}\text{Fm}(\text{sf})$  events were measured. For  $^{260}\text{[104]}$  300 events were recorded with 41  $^{256}\text{Fm}$  events. The  $^{256}\text{Fm}$  spontaneous fission activity with a half life of 2.63 h which is simultaneously produced, represents the disturbing background.

The half-lives of the  $^{258}\text{Md}$ ,  $^{259}\text{Md}$  and  $^{260}\text{Md}$  nuclides are sufficiently long to allow off-line mass separation of isotopically pure sources. These Md-isotopes were produced by transfer reactions in the bombardments of a  $^{254}\text{Es}$  target with beams of 105 MeV  $^{18}\text{O}$  and 126 MeV  $^{22}\text{Ne}$ . The recoil products were trapped in Ta-foils. The key technique was in the off-line mass separation, freeing the Md-isotopes from the  $^{256}\text{Fm}$  isotopes. The fission fragment energies were then measured in sandwiched surface barrier detectors. The 60 min  $^{258}\text{Md}$  decays by electron capture to  $^{258}\text{Gd}$  which decays further with a half-life of 380  $\mu\text{s}$  by spontaneous fission.

The experimental achievement lies here really in the production of the spontaneously fissioning heavy isotopes in pure form. This achievement was only possible due to the continuous and longstanding experience of this group.

### 2.2. Target preparation of the 26 min $^{235}\text{U}$ isomer.

$^{235}\text{U}$  has an isomeric  $1/2^+$  level with an excitation energy of 76.8 eV above the ground state level with spin and parity of  $7/2^-$ . This meta-stable state of  $^{235}\text{mU}$  decays with a half-life of 26 minutes to the ground state by means of a strongly internally converted E3 transition. The neutron captures of  $^{235}\text{U}$  and of  $^{235}\text{mU}$  lead to  $3^-$  and  $4^-$  levels and to  $0^+$  and  $1^+$ -levels near the neutron binding energy of  $^{236}\text{U}$ , respectively. Therefore, the study of the  $^{235}\text{mU}$  neutron induced fission reaction is interesting, since it gives the possibility of comparing for the same nucleus the characteristics of the fission process for states which are substantially different in their spins and parities at the same excitation energy.

The major difficulty in studying the  $^{235}\text{mU}(n,f)$  reaction is the target preparation. The production of  $^{235}\text{mU}$  nuclei and the preparation of targets of this nuclide are possible via the  $\alpha$ -decay of  $^{239}\text{Pu}$  which populates exclusively the  $1/2^+$  isomeric level of  $^{235}\text{mU}$ . The  $^{235}\text{mU}$  recoils have an energy of about 90 keV and a small positive charge. Therefore, they can be trapped on a target. The  $^{239}\text{Pu}$ -mother source should be thin, homogeneous and of a relatively large area to obtain a sufficient number of escaping  $^{235}\text{mU}$  recoils. Pauwels et al./4/ conceived and realized at CBNM-Geel the mother source in the form of a 40 cm diameter Al-sphere internally coated with  $\approx 10 \mu\text{g}/\text{cm}^2$   $^{239}\text{PuF}_3$  by vacuum deposition. Fig. 2 shows the experimental collection set-up for  $^{235}\text{mU}$  nuclei. The sphere /A/ is evacuated to 1 Pa. A lock chamber /B/ is connected, containing an electrically isolated and movable target holder /C/. An electric voltage of up to -5 kV can be applied to the target holder in order to guide the  $^{235}\text{mU}$  recoils to the target. The lock chamber

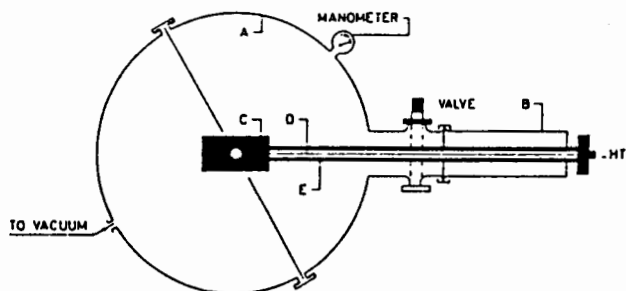


Fig. 2. The set-up for  $^{235}\text{U}$  target preparation

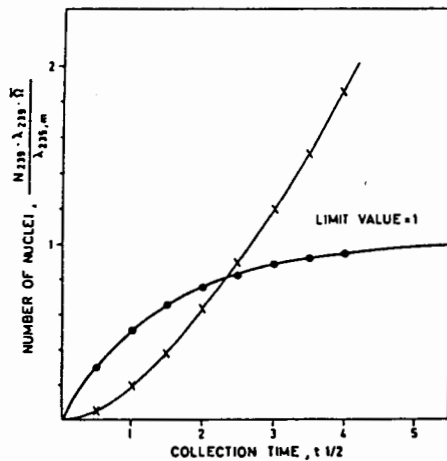


Fig. 3. Number of collected  $^{235}\text{mU}$  and  $^{235}\text{gU}$  nuclei as function of collection time

permits an exchange of targets. Fig. 3 shows the number of  $^{235}\text{mU}$  nuclei, full points, and the ingrowth of  $^{235}\text{gU}$  nuclei, crosses, as function of collection time. After one half-life  $8 \cdot 10^9$   $^{235}\text{mU}$  nuclei were collected. This was sufficient for D'Eer et al./5/ to measure at the ILL-reactor at Grenoble the fission cross section ratio of  $^{235}\text{gU}(n,f)$  to  $^{235}\text{mU}(n,f)$  at 5 meV and 28 meV incident neutron energies.

### 3. Techniques for fission fragment measurements.

In this section a selection of techniques is reviewed where fission fragment characteristics are determined.

#### 3.1. Lohengrin and a $\Delta E$ -E ionization chamber.

The Lohengrin spectrometer of the Institute Laue-Langevin in Grenoble is a well-known instrument and in operation since many years. It will, therefore, not be described here. However, it has been used by Armbruster et al./6/ in connection with a  $\Delta E$ -E ionization chamber, which permitted the identification of the new neutron rich isotopes  $^{70-74}\text{Ni}$  and  $^{74-77}\text{Cu}$  in the thermal neutron induced fission of  $^{235}\text{U}$ . The Lohengrin spectrometer sorts the fission fragments with respect to their  $A/q$  and  $E/q$ -values, where  $A, E$  and  $q$  are the mass, kinetic energy and ionic charge of the fragment, respectively. The fragments sorted for fixed pairs of  $A/q$  and  $E/q$  by Lohengrin enter an ionization chamber with

Frisch grid which measures  $\Delta E$  and the residual fragment energy. Assuming about equal incident fragment energy, the elements with lower nuclear charge number  $Z$  have the smaller energy losses and thus the nuclear charge  $Z$  can be determined. Of course, the ionization chamber must be conceived for optimum charge sensitivity in the energy-, and mass-range of fission fragments. For masses ranging from  $A = 70$  to  $A = 77$ , the partial  $\Delta E$ -E scatter plots of the elements observed in a succession of exposures are gathered in fig. 4. The  $A$ -,  $E$ -, and  $q$ -values are indicated below each single scatter plot together with the exposure time. In vertical direction the nuclear charge dependence as measured by the ionization chamber is indicated.

#### 3.2. Double velocity, velocity-energy and double energy experiments.

All three types of experiments were performed in earlier works and can be found in the literature. Here especially set-ups with surface barrier detectors and twin ionization chambers are meant, which are considered as kind of standard techniques now. However the state of the art has developed with time and one of the most up-to-date spectrometers is Cosi-Fan-Tutte at Grenoble, which was conceived by Gönnerwein et al. /7,8,9/.

The concept is shown in fig. 5. In the center of the assembly the fission layer is positioned. The fission fragment traverses a start and a stop detector for the velocity measurement and enters finally the axial ionization chamber which gives a measure of the fragment energy. The flight path length is 107 cm. In the two upper parts of fig.6

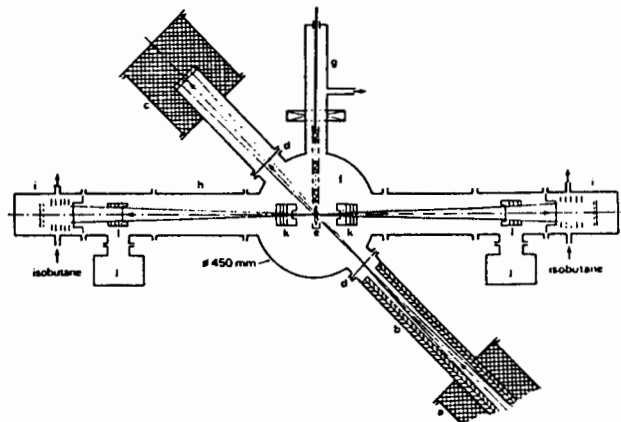


Fig. 5. Cosi-Fan-Tutte spectrometer

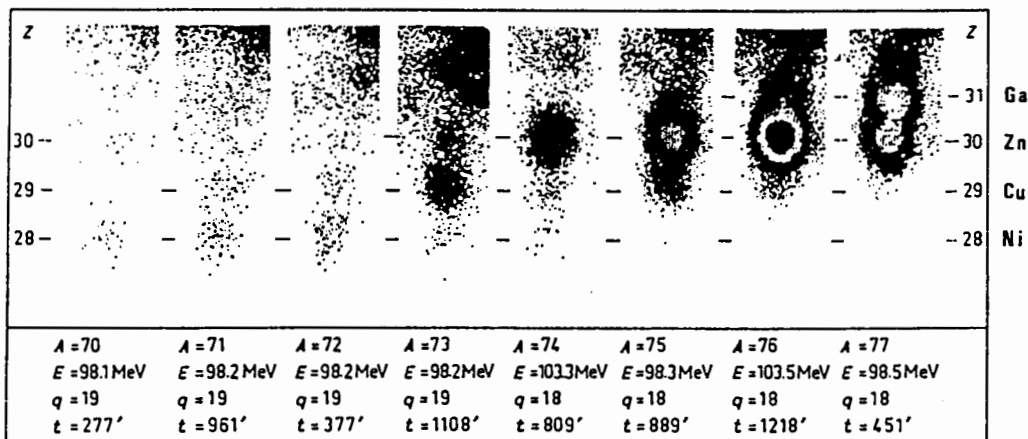


Fig. 4. Scatter plots of observed elements identified by energy loss, ref. 7

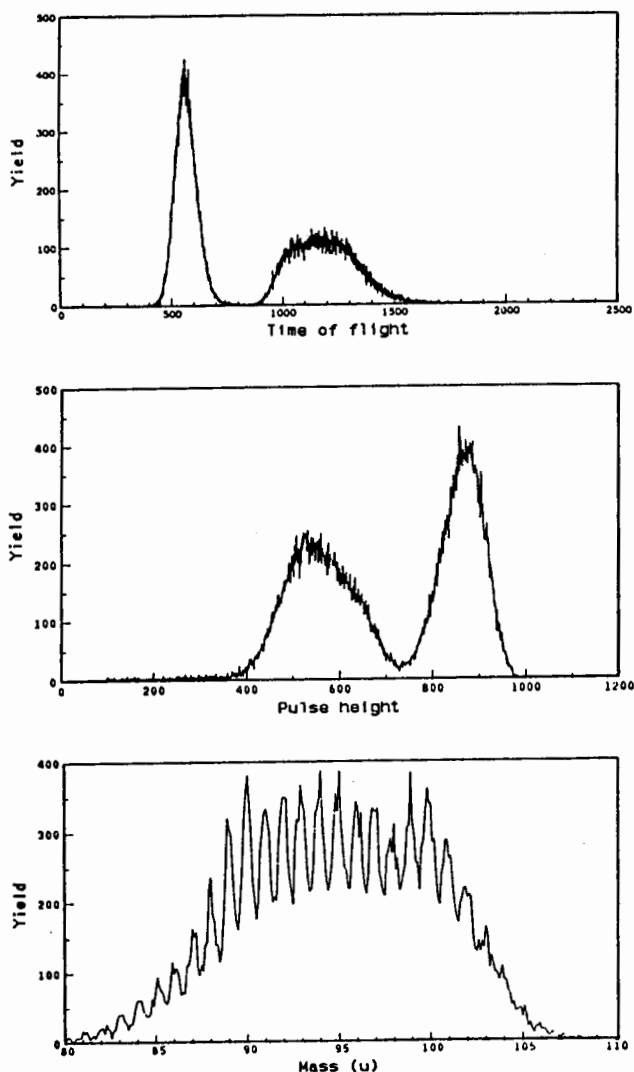


Fig. 6. Fission fragment time-of-flight-, pulse height-, and mass spectrum measured with Cosi-Fan-Tutte/9/.

the time-of-flight and the pulse height spectra are shown which were measured by Schillebeeckx et al. /10/ for thermal neutron induced fission of  $^{235}\text{U}$ . In the lowest part of fig. 6 the corresponding mass distribution is given. A mass resolution of  $\delta m/m = 0.7\%$  is obtained. The nominal energy and velocity resolutions are 0.5% and 0.2%, respectively. This detector has also the potential of obtaining information about the nuclear charge of the fragments from the ionization chamber signals as proposed by Oed et al. /8/.

#### 4. Experiments measuring fragments and other fission parameters.

##### 4.1. Photo-fission detector

At the University of Gießen, Wilke /11/ constructed a 4 $\pi$ -photo-fission detector for in-beam operation. The concept of this detector is shown in fig. 7. In the centre of the assembly the two inner detectors sandwich the fissile target, which has an area of 7 cm x 10 cm. The two hemispheres are covered by a pyramidal struc-

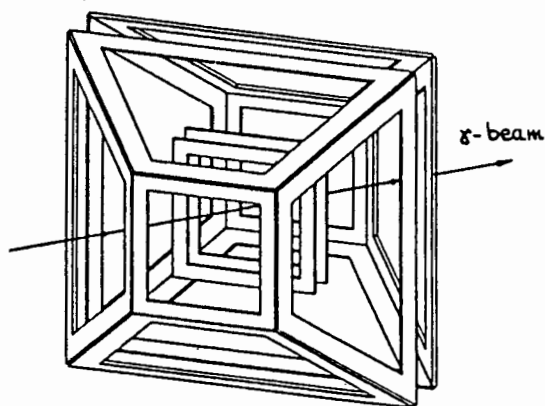


Fig. 7. Fission fragment detector arrangement for photon induced fission/11/.

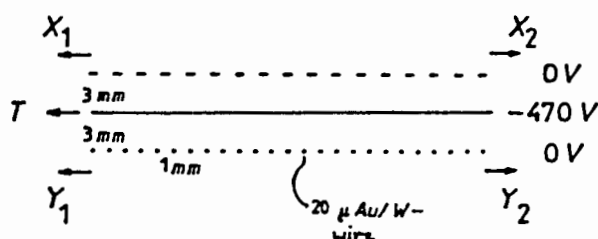


Fig. 8. Schematic view of avalanche detector, which gives timing and x- and y-coordinate.

ture where the five side areas are made of detectors. In total twelve detectors form the whole assembly. The areas of the four quadratic and eight trapezoidal detectors are 64 cm<sup>2</sup> and 128 cm<sup>2</sup>, respectively. The principle of the detectors is shown in fig. 8. They are avalanche detectors producing one timing signal and two position signals, one for each orthogonal axis. For the registration of a fission fragment, coincidence between the two central detectors and one outside detector, in one of the hemispheres, is demanded. The four position signals obtained for each fragment permit the flight path length determination as well as the determination of the angle with respect to the incident  $\gamma$ -beam. The timing and position signals together allow a mass distribution measurement. Angular distributions are measured as function of fragment mass and photon end energy. Angular distribution measurements for symmetric and asymmetric mass splits from photo-fission of  $^{238}\text{U}$  at 12.133 MeV end energy of the Bremsstrahlung spectrum gave different results /11/. This mass dependence of the angular distribution is a new result.

##### 4.2. Diogenes, detector for correlation measurements between fission fragments and light charged particles.

The double torus ionization chamber "Diogenes" is a spectrometer for correlation measurements between fission fragments and light ternary charged particles which was designed by Mutterer et al. /12,13/. Fig. 9 shows a schematic cut through this detector. The neutron beam tube passes the chamber vertically with respect to the

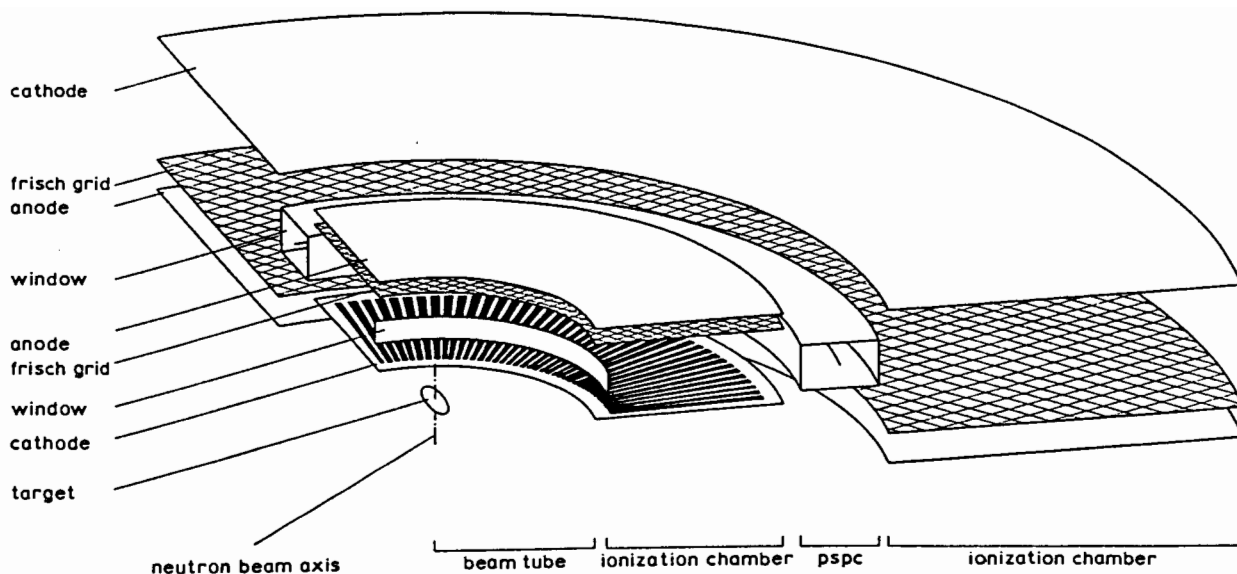


Fig. 9. Diogenes/12,13/

electrode planes. The fission fragments are completely stopped and their energies and angular directions are measured in the first toroidal Frisch-gridded ionization chamber with sectorial divisions of the cathode. The light ternary particles have a much longer range than the fission fragments. They enter, after passage of the inner, low pressure fission fragment chamber a  $\Delta E$ -E telescope, which is composed of an annular position-sensitive  $\Delta E$  proportional counter and a toroidal high pressure ionization chamber. This detector permits the measurement of the angle between the light particle- and the fission fragment path directions, an energy measurement of the light particle and a particle identification. From these kinetic parameters the main fragment masses can be obtained and the event yields can be determined as function of the mentioned parameters.

In order to indicate the kind of results which can be obtained with this complex instrument, some correlation plots of ternary fission measurements for  $^{235}\text{U}(n,f)$  induced by thermal neutrons /12/ are shown in fig. 10 between the fission fragment mass ratio on the one side and the alpha energy, and the alpha emission angle with respect to the light fragment path direction on the other. Also other cuts can be made into the multi-dimensional fission yield.

The system was also used to determine the probability for real ternary fission into three almost equal fragments /14/. An upper limit value of  $8 \cdot 10^{-8}$  per binary fission event was obtained.

#### 4.3. Correlation measurements between fission fragments and neutrons.

The first comprehensive measurement of this type was performed by Bowman et al./15/ in 1962 on the spontaneous fission of  $^{252}\text{Cf}$ . They measured the flight times of both fission fragments in a space fixed direction and also the flight-time of the neutrons. The neutron emission angle with respect to the flight path direction of the light fission fragment had to be fixed by

successively placing the neutron detector in different angular positions. The detectors were scintillators mounted on photo multipliers. A similar experiment was reported later by Piksaikin et al. /16/ and Serigina et al. /17/ who used two

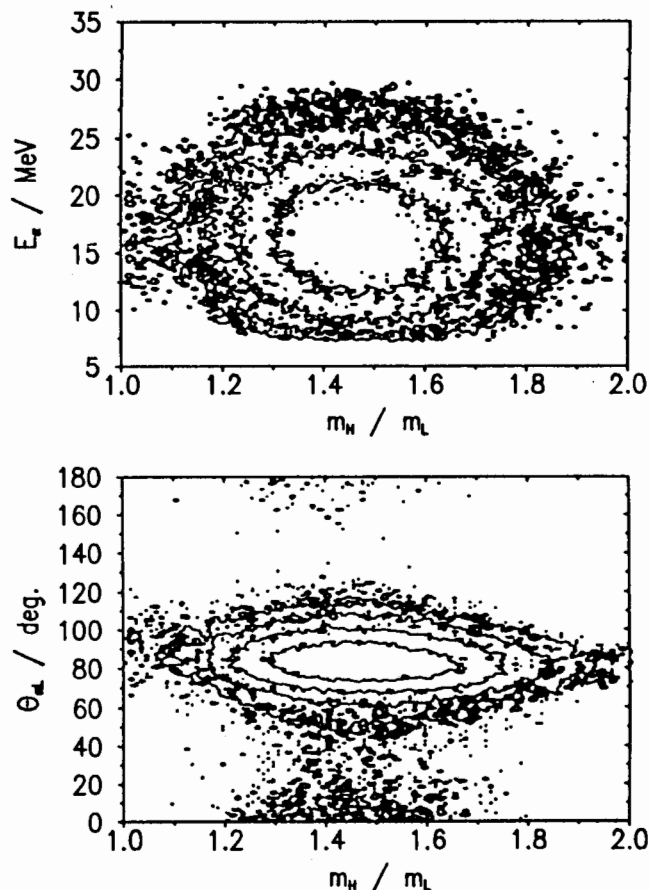


Fig. 10. Correlation plots between the fragment mass ratio and the  $\alpha$ -energy,  $E_\alpha$ , and the angle between the directions of motions of the light fragment and the alpha particle.

surface-barrier detectors for double energy measurements and a stilbene scintillation detector, operated as a proton recoil spectrometer for neutron energy and angle measurements. Also here the neutron detector had to be moved from one angular position to another.

Märten et al./18/ presented recently a set-up of two parallel plate avalanche detectors, where one of them is position-sensitive for fission fragment velocity and direction measurements. The geometrical arrangement is shown in fig. 11. The neutron time-of-flight detector N1 with pulse-shape discrimination permits the measurement of the correlations with the neutrons. One advantage of this set-up is that no detector movement is needed for the angular distribution measurement. The disadvantage is however, that energy or flight-time of the second fragment is not measured and therefore an important parameter of the kinematics of the fission process is missing.

Another set-up for correlation measurements between fission fragments and neutrons was published in several papers by Budtz-Jørgensen et al./19, 20, 21, 22/. The experimental set-up is shown in fig. 12. The fission fragment detector is a twin ionization chamber which permits the

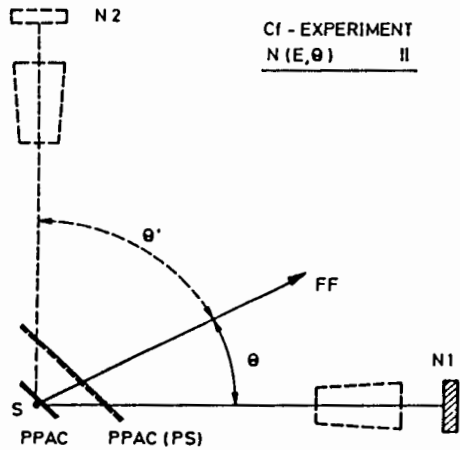


Fig. 11. Schematic plot of a neutron fragment correlation experiment/18/.

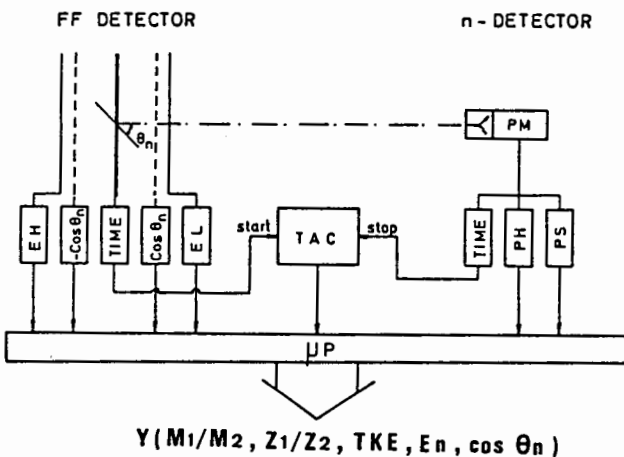


Fig. 12. Experimental set-up for fission fragment and neutron correlation measurements.

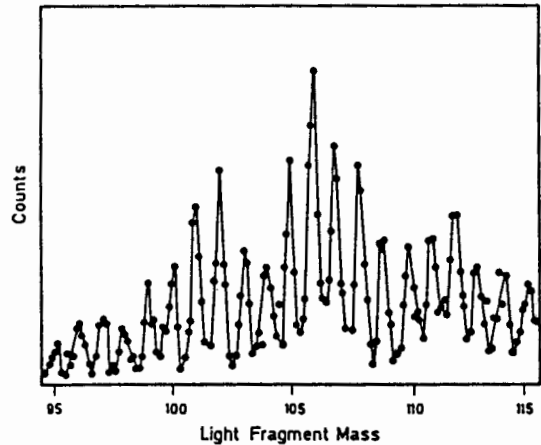


Fig. 13.  $^{252}\text{Cf}(\text{SF})$  light fragment mass distribution for high TKE-values.

measurement of the energies of both fragments, their emission angle with respect to the normal on the electrodes, and their nuclear charge ratio distribution. From the common cathode, which contains the fission source, a timing signal with a time jitter of less than 0.7 ns is obtained which is used for neutron time-of-flight measurements. The neutron detector positioned on the symmetry axis of the twin chamber permits then to measure the neutron flight-time, in coincidence with the fission fragment parameters obtainable from the twin chamber. Since the fission chamber works in an advantageous  $4\pi$ -geometry, the angular correlations can be measured simultaneously, covering the whole angular range.

In order to show the capabilities of this experimental technique, some cuts through the fission yield of  $^{252}\text{Cf}(\text{SF})$  as function of fragment mass, total kinetic energy, nuclear charge ratio, fission neutron energy and fission neutron emission angle are presented.

Fig. 13 shows a part of the light fragment mass distribution for fragment energies by 27 MeV larger than the average energy as function of mass split. A mass resolution of  $<0.4$  u is observed. Fig. 14 shows the nuclear charge distribution for isobaric fission fragments with a total kinetic

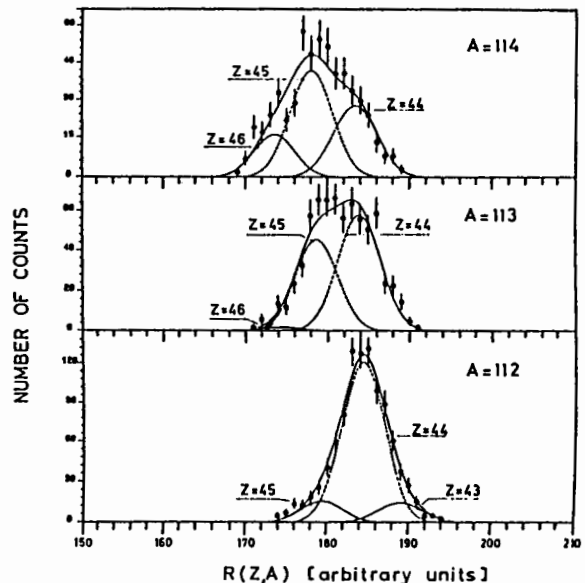


Fig. 14. Nuclear charge distributions for fission fragment isobars.

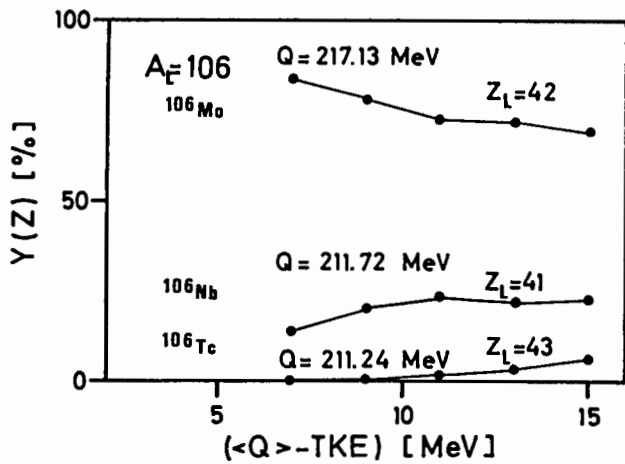


Fig. 15. Elemental yield of isobar 106 as function of  $\langle Q \rangle$ -value minus fragments total kinetic energy TKE.

energy of 27 MeV above the average energy. The width of the nuclear charge distribution changes considerably with the isobar. The relative experimental charge width for one nuclide  $\sigma(Z_L, A_1)/R$  was found to be 1.45% for  $38 \leq Z \leq 48$ . Although, the charge resolution does not allow a complete separation of individual nuclear charges, it is sufficient for the determination of charge distributions in fission.

Fig. 15 shows the dependence of the nuclear charge partition from the total kinetic energy of the fragments near the reaction Q-value for the isobar 106.

The measurements of the nuclear charge and mass in the spontaneous fission of  $^{252}\text{Cf}$  permitted without special effort the straight forward identification of 40 nuclides lying outside the range of the Karlsruhe chart of nuclides as published in 1981. These nuclides are listed in table 1.

With the present experimental set-up one can measure the fission neutron spectra as function of fragment mass, total kinetic energy and emission angle. As one example a biparametric plot of the number of fission events as function of fission neutron energy and of the cosine of the angle between the directions of motion of the light fragment and the neutron is shown in fig. 16. The present experiment also permits to evalu-

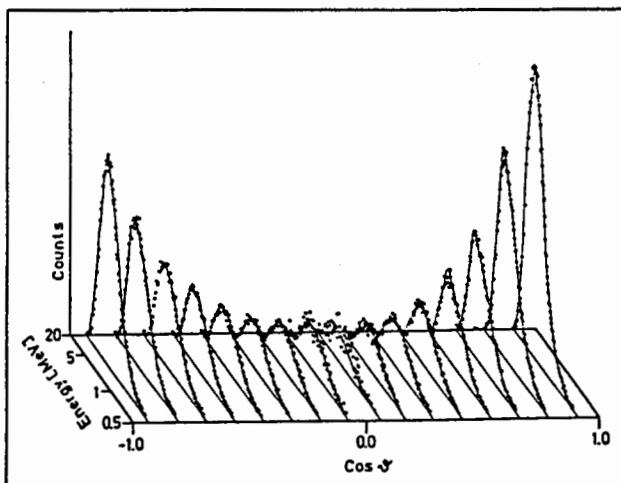


Fig. 16. Biparametric plot of fission yield as function of fission neutron energy and  $\cos \alpha$

Table 1.: Neutron rich nuclides outside the Karlsruhe Chart of Nuclides identified with twin ionization chamber from  $^{252}\text{Cf}(\text{sf})$

Z				
36	$^{96}\text{Kr}$			
39	$^{103}\text{Y}$			
40	$^{105}\text{Zr}$	$^{106}\text{Zr}$		
41	$^{107}\text{Nb}$	$^{108}\text{Nb}$	$^{109}\text{Nb}$	
42	$^{109}\text{Mo}$	$^{110}\text{Nb}$	$^{111}\text{Mo}$	$^{112}\text{Mo}$
43	$^{111}\text{Tc}$	$^{112}\text{Tc}$	$^{113}\text{Tc}$	
44	$^{114}\text{Ru}$	$^{115}\text{Ru}$	$^{116}\text{Ru}$	
45	$^{115}\text{Rh}$	$^{116}\text{Rh}$	$^{117}\text{Rh}$	
46	$^{119}\text{Pd}$	$^{120}\text{Pd}$	$^{121}\text{Pd}$	
56	$^{149}\text{Ba}$			
57	$^{150}\text{La}$	$^{151}\text{La}$	$^{152}\text{La}$	$^{153}\text{La}$
58	$^{152}\text{Ce}$	$^{153}\text{Ce}$	$^{154}\text{Ce}$	
59	$^{152}\text{Pr}$	$^{153}\text{Pr}$	$^{154}\text{Pr}$	$^{155}\text{Pr}$
60	$^{155}\text{Nd}$	$^{156}\text{Nd}$	$^{157}\text{Nd}$	
61	$^{155}\text{Pm}$	$^{156}\text{Pm}$		

ate the average number of neutrons,  $\bar{\nu}$ , as function of mass and total kinetic energy. Fig. 17 shows  $\bar{\nu}$  as function of mass split only. Due to the  $3 \cdot 10^6$  measured fission fragment neutron coincidences and the  $100 \cdot 10^6$  fission fragment events measured without neutron coincidences, it was possible to extend the  $\bar{\nu}$ -measurements considerably in their mass range compared to earlier measurements. In fig. 17 the experimental data below mass 82 show an increase in  $\bar{\nu}$ , indicating an additional saw-tooth. The  $N = 50$  shell closure is reached at mass 82. At the heavy mass end, above mass 176, a clear decrease of the neutron multiplicity is observed producing a third saw-tooth. The full line is a prediction for  $\bar{\nu}$ , the neutron multiplicity, made by Brosa et al /23/.

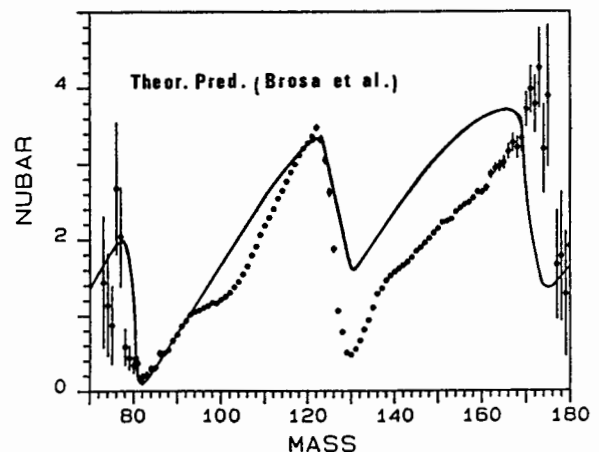


Fig. 17. Neutron multiplicity of  $^{252}\text{Cf}(\text{sf})$  as function of fragment mass.

The presently presented twin chamber was used also in the beam of GELINA to measure fragment mass-, and TKE-distributions for isolated resonances of  $^{235}\text{U}(n,f)/24/$ .

#### REFERENCES

- 1) E.K. Hulet, J.F. Wild, R.J. Dougan, R.W. Loughheed, J.H. Landrum, A.D. Dougan, M. Schädel, R.L. Hahn, P.A. Baisden, C.M. Henderson, R.J. Dupzyk, K. Sümmerer, and G.R. Bethone  
Phys. Rev. Let. 56, 313(1986)
- 2) J.M. Nitschke, M. Fowler, A. Ghiorso, R.E. Leber, M.E. Leino, M.J. Nurmia, L.P. Somerville, K.E. Williams, E.K. Hulet, J.H. Landrum, R.W. Loughheed, J.F. Wild, C.E. Bemis, J.R. Silva, and P. Eskola  
Nucl. Phys. A352, 138(1981)
- 3) L.P. Somerville, M.J. Nurmia, J.M. Nitschke, A. Ghiorso, E.K. Hulet, and R. W.L. Loughheed  
Phys. Rev. C31, 1801(1985)
- 4) J. Pauwels, R. Eykens, A. D'Eer, C. Wagemans, and M. Nève de Mevergnies  
Nucl. Instr. Meth. A257, 21(1987)
- 5) A. D'Eer, C. Wagemans, M. Nève de Mevergnies, F. Gönnerwein, P. Geltenbort, M. S. Moore, J. Pauwels  
submitted to Phys. Rev. C.
- 6) P. Armbruster, M. Bernas, J.P. Bocquet, R. Brissot, H.R. Faust, and P. Roussel  
Europhys. Lett. 4, 793(1987)
- 7) A. Oed, G. Barreau, F. Gönnerwein, P. Perrin, and C. Ristori  
Nucl. Instr. Meth. 179, 265(1981)
- 8) A. Oed, P. Geltenbort, and F. Gönnerwein  
Nucl. Instr. Meth. 205, 451(1983)
- 9) A. Oed, P. Geltenbort, F. Gönnerwein, T. Manning, and D. Souque  
Nucl. Instr. Meth. 205, 455(1983)
- 10) P. Schillebeeckx, C. Wagemans, P. Geltenbort, A. Oed and F. Gönnerwein  
Proc. of the Seminar on Fission, Castle of Pont d'Oye, Habay-la-Neuve, Belgium, 22nd-23rd May, 1986, SCK-Mol, BGL-586, page 130(1986)
- 11) W. Wilke  
Ph.-D. Thesis (1987),  
Justus-Liebig-Universität, Giessen, Germany
- 12) J.P. Theobald  
Proc. of the Seminar on Fission, Castle of Pont d'Oye, Habay-la-Neuve, Belgium, 22nd-23rd May 1986, 1040 Brussel, E. Plasky laan 144, BLG-586, page 63
- 13) P. Heeg, K.F. Hoffmann, M. Mutterer, J.P. Theobald, K. Weingärtner, J. Pannicke, F. Gönnerwein, G. Barreau, and B. Leroux  
Nucl. Phys. A409, 379(1983)
- 14) Patricia Schall, P. Heeg, M. Mutterer, and J.P. Theobald  
On symmetric tripartition in the spontaneous fission of  $^{252}\text{Cf}$ , IKDA 87/4, Institut für Kernphysik, Technische Hochschule Darmstadt (1987)
- 15) H.R. Bowman, S.G. Thompson, J. C.D. Milton, and W.J. Swiatecki  
Phys. Rev. 126, 2120(1962)
- 16) V.M. Piksaikin, P.P. D'Yachenko, and L.S. Kutsaeva  
Yad. Fiz. 25, 723(1977)
- 17) E.A. Seregina, and P.P. D'Yachenko  
Yad. Fiz. 42, 1337 (1985)
- 18) H. Märten, D. Richter, D. Seeliger, W.D. Fromm, W. Neubert, and A. Lajtai  
Nucl. Instr. Meth. A264, 375(1988)
- 19) C. Budtz-Jørgensen, and H.-H. Knitter  
Proc. of Symposium on Nuclear Fission, Nov. 1985, Gaussig/Dresden
- 20) C. Budtz-Jørgensen, H.-H. Knitter, Ch. Straede, and F.-J. Hamsch  
Proc. of Workshop on Nuclear Dynamics 4, 24th-28th February 1986, p.17, Copper Mountain, Colorado USA(1986)
- 21) C. Budtz-Jørgensen, and H.-H. Knitter  
Proc. of the Seminar on Fission, Castle of Pont d'Oye, Habay-la-Neuve, Belgium, 22nd-23rd May 1986, BLG-586, page 91(1986)
- 22) C. Budtz-Jørgensen, H.-H. Knitter, Ch. Straede, F.-J. Hamsch, and R. Vogt  
Nucl. Instr. Meth. A258, 209(1987)
- 23) U. Brosa  
to be published in Phys. Rev. C
- 24) H.-H. Knitter, F.-J. Hamsch, C. Budtz-Jørgensen and J.P. Theobald  
Proc. of Intern. Conf. on Neutron Physics, Kiev, SU, Sep. 1987